

• 专题研究:肿瘤 •

PARP1在K192位点的乳酸化抑制卵巢癌细胞的迁移和增殖

苏宁¹, 曹颖^{2,3}, 张淑平¹, 吴少君⁴, 孙鸿展⁴, 唐雪俊², 袁冬兰⁴, 张东^{1*}, 杨莉莉^{4*}, 应小燕^{2*}

¹南京医科大学生殖医学与子代健康全国重点实验室, 江苏 南京 211166; ²南京医科大学第二附属医院妇科, 江苏 南京 210029; ³连云港市妇幼保健院妇科, 江苏 连云港 222000; ⁴南京医科大学附属泰州人民医院妇科, 江苏 泰州 225300

[摘要] 目的: 卵巢癌(ovarian cancer, OC)在全球女性癌症中排名前列。许多研究在多个遗传调控水平上探究了OC的发生和进展。但很少有研究探讨翻译后修饰(post-translation modification, PTM)对OC进展的影响, 而这对发现新的治疗靶点至关重要。本研究拟通过系统鉴定OC进展的关键PTM类型, 探讨并评估其在治疗靶点的转化潜力。方法: 首先, 利用多种泛PTM抗体来比较临床女性正常卵巢组织和OC组织之间的泛PTM水平。在鉴定出乳酸化为差异最显著的PTM后, 选择代表性的样品进行无标记质谱分析, 以识别特定的乳酸化位点。随后用野生型(wild type, WT)PARP1-EGFP-STREP II或其K192A突变体转染A2780卵巢癌细胞, 检测与增殖(克隆形成实验)、ROS水平和迁移(细胞划痕实验)相关的各种细胞指标。结果: 临床OC样本中的泛乳酸化水平显著上调, 其中PARP1在K192位点的乳酸化是变化最为显著的PTM之一。PARP1-WT的过表达能显著抑制OC细胞系A2780的生长和迁移活性, 而K192A突变体则失去了这种抑制作用。此外, PARP1-WT过表达可显著下调ERK1/2信号通路的磷酸化水平。结论: 本研究发现并证实了OC中存在PARP1的新型PTM形式——乳酸化修饰, K192位点的乳酸化通过ERK1/2途径调节OC细胞的生长和迁移。

[关键词] PARP1; 乳酸化; 迁移; 增殖; 卵巢癌细胞

[中图分类号] R737.31

[文献标志码] A

[文章编号] 1007-4368(2025)09-1219-11

doi: 10.7655/NYDXBNSN241251

Lactylation of PARP1 at K192 inhibits the migration and proliferation of ovarian cancer cells

SU Ning¹, CAO Ying^{2, 3}, ZHANG Shuping¹, WU Shaojun⁴, SUN Hongzhan⁴, TANG Xuejun², YUAN Donglan⁴, ZHANG Dong^{1*}, YANG Lili^{4*}, YING Xiaoyan^{2*}

¹State Key Laboratory of Reproductive Medicine and Offspring Health, Nanjing Medical University, Nanjing 211166;

²Department of Gynecology, the Second Affiliated Hospital of Nanjing Medical University, Nanjing 210029;

³Department of Gynecology, Lianyungang Maternal and Child Health Hospital, Lianyungang 222000; ⁴Department of Gynecology, Taizhou People's Hospital Affiliated to Nanjing Medical University, Taizhou 225300, China

[Abstract] **Objective:** Ovarian cancer (OC) ranks among the leading causes of mortality among the female cancers worldwide. Numerous studies have explored the development and progression of OC at multiple genetic regulatory levels. However, relatively few studies have explored the impact of post-translational modifications (PTM) on OC progression, which is essential for uncovering new therapeutic targets. This study aimed to systematically identify the key PTM types involved in OC progression, and to explore and evaluate their translational potential as therapeutic targets. **Methods:** First, we utilized multiple general PTM antibodies to compare gross PTM levels between normal ovarian and OC tissues from clinical females. After identifying lactylation as the PTM with the most significant differences, we selected representative samples for label-free mass spectrometry to identify specific lactylation sites. Next, we transfected A2780 (OC) cells with either wild-type (WT) or mutant (K192A [Q]) poly (ADP-ribose) polymerase 1 (PARP1) conjugated to enhanced green fluorescent protein (EGFP) with a Strep II peptide tag and assessed various cellular indexes related to cell proliferation (clonogenicity assay), migration (scratch wound healing assay), and reactive oxygen species levels. **Results:** Pan-

[基金项目] 国家自然科学基金(32070840, 32370912); 江苏省妇幼健康重点学科基金(FXK201712)

*通信作者(Corresponding author), E-mail: xiaoyanying_cool@163.com (ORCID: 0000-0003-0326-4987); elevenfox007@njmu.edu.cn (ORCID: 0009-0001-1584-2417); dong.ray.zhang@njmu.edu.cn (ORCID: 0000-0002-0257-4441)

lactylation was significantly upregulated in clinical OC samples, with PARP1 lactylation at K192 being one of the most common modifications. The growth and migration of A2780 cells were markedly suppressed by overexpressing PARP1-WT but not mutant PARP1. Overexpressing PARP1 significantly downregulated the phosphorylation of extracellular signal-regulated kinases 1/2 (ERK1/2). **Conclusion:** This study uncovered a novel PTM of PARP1 in OC, lactylation, and demonstrated that lactylation at K192 is crucial in regulating OC cell growth and migration *via* the ERK1/2 pathway. Further investigations are required to elucidate the broader functional implications of PARP1 lactylation and its therapeutic potential.

[Key words] PARP1; lactylation; migration; proliferation; ovarian cancer cells

[J Nanjing Med Univ, 2025, 45(09): 1219-1228, 1241]

Ovarian cancer(OC) ranks the third most common cancer among women and the leading cause of cancer-related mortality in gynecological cancers, with over 22 000 women diagnosed and approximately 14 000 dying from OC annually in the United States^[1]. Early diagnosis of OC is challenging, primarily due to its subtle initial symptoms, such as bloating, indigestion, lower back pain, and frequent urination, which are often mistaken for other benign conditions^[2], leading to diagnostic delays. As a result, over 70% of OC cases are diagnosed at an advanced stage. Late diagnosis often leaves patients with limited treatment options and a poor prognosis^[3]. While OC has several subtypes, its treatment remains relatively consistent, primarily involving tumor debulking surgery and platinum-based combination chemotherapy with taxanes^[4]. Although OC is considered as a platinum-sensitive tumor with a high response rate to first-line standard treatment, 75% of patients with advanced OC will still experience metastasis, recurrence, and ultimately resistance, resulting in poor long-term survival. Discovering new biomarkers associated with OC is crucial for improving treatment outcomes for patients with this disease.

Post-translational modifications(PTMs), which involve the covalent modification of amino acids within proteins, have been shown to play crucial roles in numerous cellular processes^[5-7]. Advances in high-throughput sequencing technologies have led to the discovery of novel PTMs, including lactylation. In 2019, Zhang et al^[8] first reported histone lactylation, which involves the addition of a lactyl group to lysine residues on histone tails. Since then, histone lactylation has been increasingly reported in various diseases, cell types, and organisms, including cancers such as non-small cell lung cancer^[9] and bladder cancer^[10], immune-related

cells like macrophages^[11], and plants^[12]. Like other PTMs, such as acetylation, methylation, phosphorylation, and ubiquitination, lactylation has been identified as another epigenetic modulator of gene expression^[8].

Poly (ADP-ribose) polymerase-1 (PARP1) is a PTM enzyme that catalyzes the removal of ADP-ribose residues from oxidized nicotinamide adenine dinucleotide (NAD⁺) to the target substrate, forming poly (ADP-ribose) (PAR). This process is essential for various cellular functions, including the repair of double-strand breaks, cell adhesion and movement, transcriptional regulation, innate immunity, and apoptosis^[13-14]. Numerous studies have shown that PARP1 levels are upregulated in diverse tumors^[15-16]. The crosstalk between acetylation, ubiquitination, and SUMOylation at multiple PARP1 sites has been implicated in the pathogenesis of neurodegenerative diseases^[17]. Moreover, PARP1 acetylation has been shown to promote nuclear factor kappa B (NF- κ B)-mediated chemoresistance to platinum compounds in cancer cells^[18]. However, studies on the lactylation of PARP1 remain scarce.

In this study, we found that lactylation was the most significantly upregulated PTM in OC samples. Using label-free mass spectrometry, we identified 10 upregulated and 16 downregulated lactylation sites within proteins that are important in multiple key cellular processes. We also demonstrated that lactylation of PARP1 at the K192 site significantly inhibits the growth and migration of OC cells by downregulating phosphorylated(p)-extracellular signal-regulated kinases(ERKs).

1 Materials and methods

1.1 Materials

1.1.1 Cell lines and cell culture

The human OC cell line, A2780 was obtained

from the China Cell Bank (Shanghai, China). The A2780 cells were cultivated in high-glucose Dulbecco's modified Eagle medium (Gibco, USA) supplemented with 10% fetal bovine serum (Gibco, USA) and 1% penicillin/streptomycin (Sigma, USA) at 37 °C in a 5% CO₂ incubator with 90% humidity.

1.1.2 Tumor samples and normal tissues

Clinical OC samples, including primary OC tissues ($n=37$) and normal ovarian tissues ($n=21$), were collected from the Second Affiliated Hospital (SAH) of Nanjing Medical University (NJMU). The tissue samples were examined by qualified clinicians to ensure the correct classification. This study was conducted in strict accordance with the 1975 Declaration of Helsinki and was approved by the Ethics Committees of the SAH of NJMU (authorization no.: [2023]-KY-007-01).

1.2 Methods

1.2.1 Dot blotting

Proteins were isolated from clinical tissue samples by lysing with PIPA buffer, separated by sodium dodecyl sulfate - polyacrylamide gel electrophoresis (SDS-PAGE), and then transferred to polyvinylidene difluoride (PVDF) membranes. Next, the membranes were washed and blocked with blocking buffer (Tris-buffered saline with Tween 20 containing 5% non-fat milk). Subsequently, they were incubated with primary and secondary antibodies against target proteins. Finally, the target proteins were visualized using an enhanced chemiluminescence (ECL) kit (Yeasen, Shanghai, China) and an ECL detection system (Tanon, Shanghai, China).

1.2.2 PTM identification by mass spectrometry

Human OC and normal ovarian tissue samples (three per group) were preserved in dry ice and transported to a specialized mass spectrometry company (BiotechPack, Beijing, China) for PTM site identification.

1.2.3 Plasmid construction and transfection

Enhanced green fluorescent protein (EGFP) with a Strep II peptide tag was attached to the C-terminal end of human PARP1 and inserted into the mammalian expression plasmid pcDNA3.1(+). The PARP1-K192A and -K192Q mutant constructs were generated by site-directed mutagenesis (Vazyme, Nanjing, China) using the wild-type (WT) plasmid as a template. A2780 cells

were transfected with empty (no PARP1 insert), PARP1-WT, or PARP1-K192A plasmids using Lipofectamine 2000 reagent (Fisher Scientific, USA). The cells were then cultured for 24 h for PARP1 expression.

1.2.4 Colony formation assays

Twenty-four hours after the transfection, 200 cells were seeded into each sub-well of a six-well plate and cultivated for additional six days. The wells were then fixed with 1% paraformaldehyde, stained with 0.1% crystal violet dye, and analyzed under a light microscope (Ti2-A, Nikon, Japan).

1.2.5 Wound healing assay

Twenty-four hours after transfection, 5×10^5 cells were seeded into each sub-well of the six-well plates and cultured until 80%–90% confluence. Next, a sterile 10 μ L pipette tip was used to create a linear scratch across the cell monolayer. Then, three randomly selected areas were imaged at assigned time points (0, 24, 48 h) using a light microscope and measured with ImageJ software.

1.2.6 ROS detection

Reactive oxygen species (ROS) were quantified using a ROS Detection Kit (Beyotime, China). First, cells were spread on glass slides and immobilized, then incubated with a ROS detection probe tagged with dichlorofluorescein diacetate for 20 min at 37 °C in the dark. Then, ROS signals were imaged under a spinning disk confocal microscope (Oxford Instruments, UK).

1.2.7 Detection of early apoptosis

A2780 cells were cultured in dishes with a glass bottom and stained with 5 μ L of an Annexin V-FITC/PI Kit (Yeasen, China) for 15 min in the dark at room temperature. Finally, apoptosis signals were imaged under a spinning disk confocal microscope.

1.2.8 Immunofluorescence

Immunofluorescence was performed as previously described^[9]. Briefly, A2780 cells were grown on glass slips and then permeated, fixed, and blocked with 1% bovine serum albumin in PHEM. Then, they were incubated with primary antibodies against marker of proliferation Ki-67 (MKI67; Cell Signaling Technology, USA) and proliferating cell nuclear antigen (PCNA; Sangon Biotech, Shanghai, China) and then relevant fluorophore-tagged secondary antibodies. DNA was

stained with 4', 6-diamidino-2-phenylindole (Beyotime, China). Cells were imaged under a spinning disk confocal microscope.

1.3 Statistical analysis

Statistical analyses were performed using GraphPad Prism (version 8.0). Each experiment was repeated at least three times. Data are presented as the mean ± standard error of the mean (SEM), without excluding maximum or minimum values. Data were compared between two groups using Student's *t*-test, and among three or more groups using one-way analysis of variance (ANOVA). *P*-value of <0.05 was considered statistically significant.

2 Results

2.1 Lactylation showed the most significant upregulation in OC

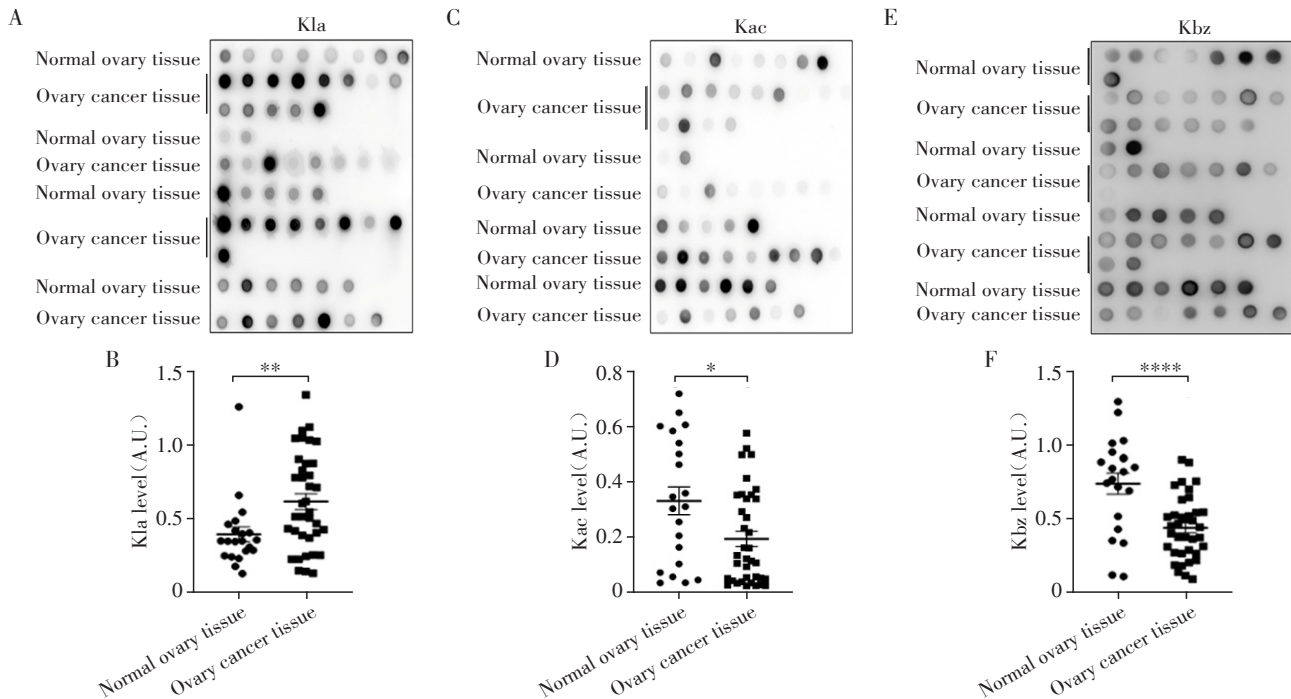
No previous studies have comprehensively compared pan-PTMs in OC. We first employed antibodies against seven PTMs (isobutyrylation, acetylation, lactylation, benzoylation, succinylation, malonylation, and

crotonylation) to compare pan-PTM levels between groups. To simultaneously analyze all examined samples (clinical normal ovarian and OC tissues) in parallel, we initially used dot blots for preliminary screening. Lactylation (Figure 1A, B), acetylation (Figure 1C, D), and benzoylation (Figure 1E, F) exhibited the most significant changes, with lactylation showing the most pronounced upregulation (Figure 1A, B), whereas acetylation and benzoylation were downregulated. Considering that an upregulated index is preferred for clinical diagnosis, we focused on lactylation.

2.2 Lactylation site identification and bioinformatics

Clinical samples are usually distinct from each other in many aspects, which is always a major issue in omics studies. We selected six control and OC samples based on the pan-lactylation dot-blot intensity and then confirmed their lactylation (Figure 2A), benzoylation (Figure 2B), and acetylation (Figure 2C) levels by Western blot.

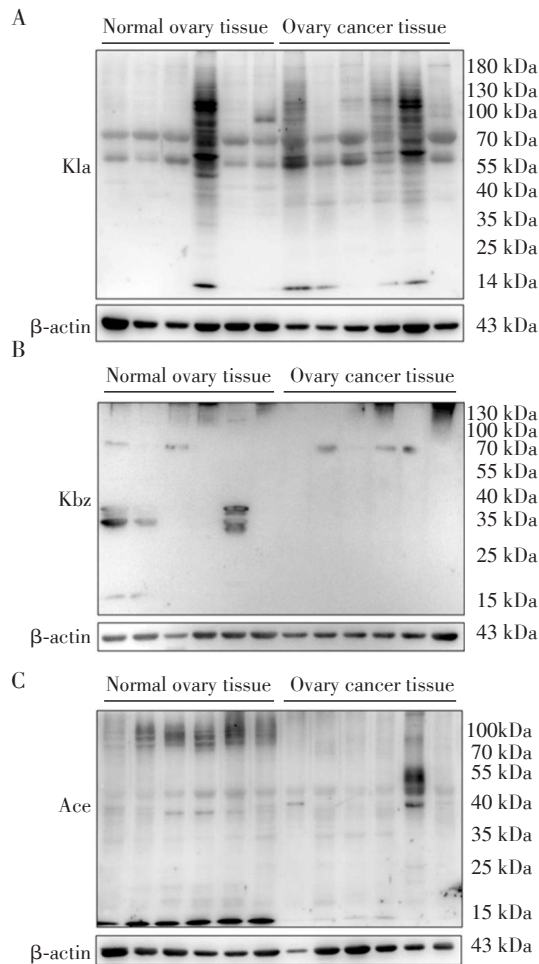
Next, we verified the tumor features of the selected tissues through blood vessel marker platelet and endo-



Dot blotting and quantification showed that the levels of pan-lactylation (A and B), pan-acetylation (C and D) and pan-benzoylation (E and F) significantly changed in clinical OC samples. Among these three pan-PTMs, pan-lactylation was the most significantly upregulated. Kla, lysine lactylation; Kac, lysine acetylation; Kbz, lysine benzoylation. **P* < 0.05; ***P* < 0.01, and *****P* < 0.001 (*n* = 21 for normal ovary tissue, *n* = 37 for ovary cancer tissue).

图1 在临床正常卵巢组织与卵巢癌组织中斑点印迹及量化有差异的泛PTMs

Figure 1 Dot blotting and quantification of the pan-PTMs with significant differences in clinical normal ovarian and OC tissues



Western blotting showed that the levels of pan-lactylation(A), pan-benzoylation(B), and pan-acetylation(C) significantly changed in clinical OC samples($n=6$).

图2 在选定的正常卵巢组织和OC组织中蛋白印迹检测有显著差异的泛PTMs

Figure 2 Western blot of pan-PTMs with significant differences in selected clinical normal ovarian and OC tissues

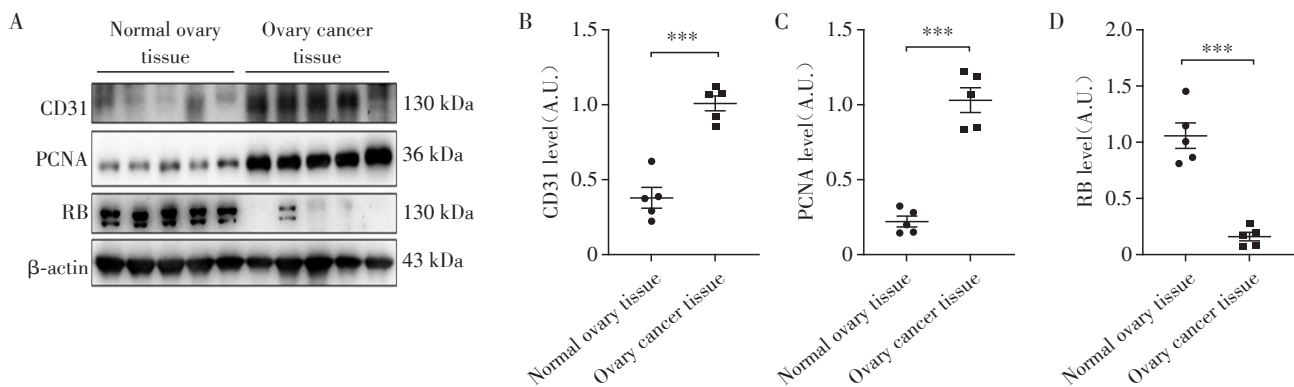
thelial cell adhesion molecule 1 (PECAM1/CD31, Figure 3A, B), proliferation marker PCNA (Figure 3A, C), and tumor suppressor marker RB transcriptional corepressor 1 (RB1, Figure 3A, D).

Then, from the upper selected samples (five per group), we randomly picked three for label-free identification of lactylation sites. We identified 10 upregulated and 16 downregulated sites (Figure 4A). Kyoto Encyclopedia of Genes and Genomes (KEGG) analysis showed that the top processes included ribosome, protein, and proteasome (Figure 4B, C).

2.3 PARP1-K192 lactylation is important for OC progression

We employed String and Cormine to analyze the interactions between upregulated and downregulated proteins, which we defined as differentially lactylated proteins (DLP). We found that PARP1 interacts multiple oncoproteins (Figure 5A). Therefore, we believed that focusing on PARP1 lactylation could serve as a good model for studying the function of lactylation in OC. PARP1 undergoes lactylation specifically at the K192 residue. Although the AlphaFold prediction did not indicate that the inactivation of K192 lactylation (K192A) significantly altered the spatial configuration of PARP1 (Figure 5B, C), we speculated that K192A might still influence PARP1's functionality.

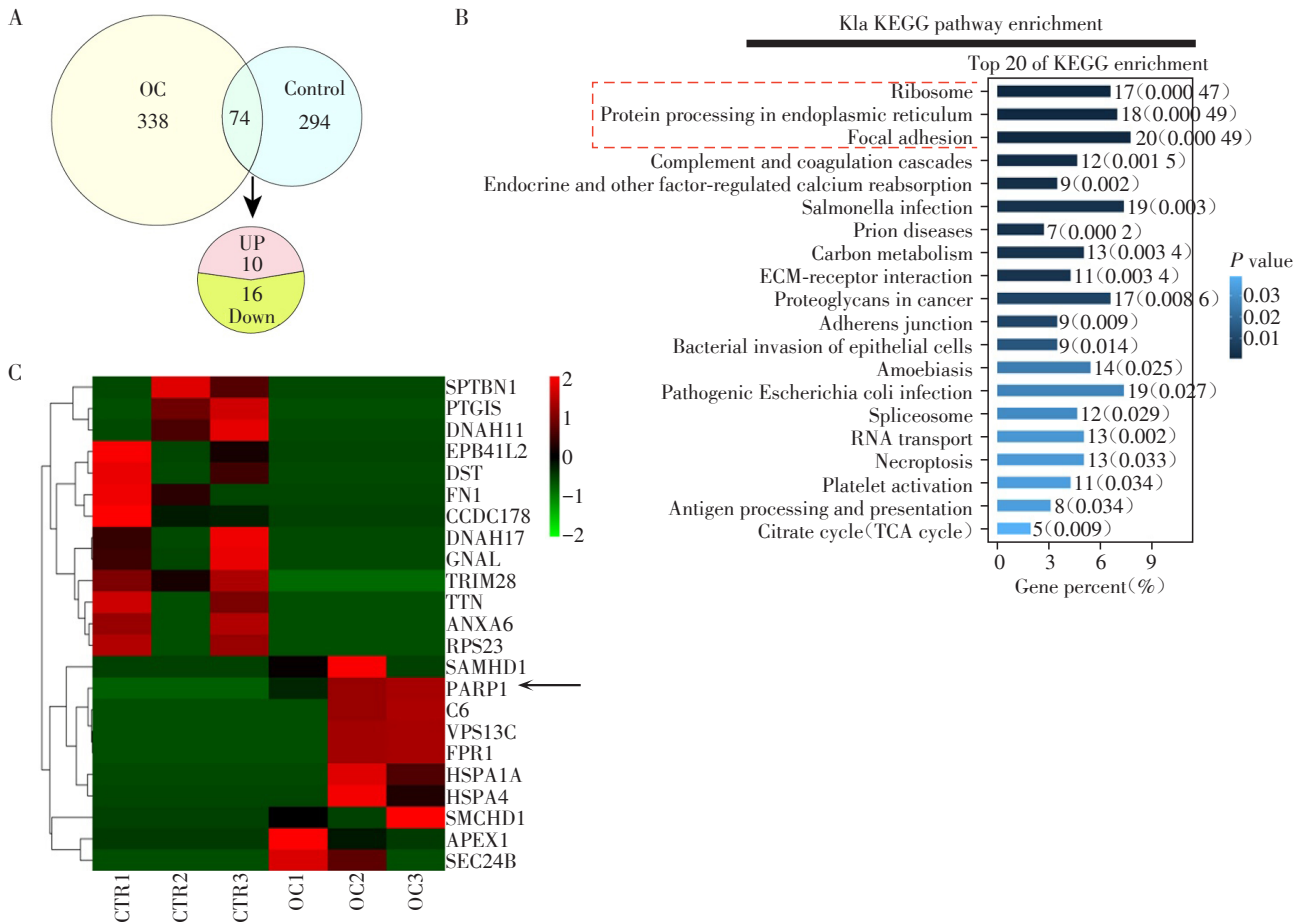
To explore this further, we overexpressed either PARP1 wild type (WT) or PARP1-K192A in A2780 cells to assess their effects. We first confirmed, through EGFP fluorescence imaging and immunoblot-



Western blotting of cancer marker genes showed that CD31 (A and B) and PCNA (A and C) significantly increased, while RB (A and D) significantly decreased. $***P < 0.001 (n=5)$.

图3 对选定的临床对照和OC样本肿瘤特征进行验证

Figure 3 Verification of the tumor character of selected clinical control and OC samples



A: Venn diagram of selected sites between clinical control and OC samples. B: Heat map of differentially-lactylated sites identified by label-free mass spec between clinical control and OC samples. C: KEGG analysis of differentially-lactylated sites ($n=3$ for each group).

图4 在临床卵巢癌样本中通过质谱鉴定蛋白的差异乳酸化位点
Figure 4 Mass spec identification of differentially-lactylated sites in clinical OC samples

ting, that both WT and K192A PARP1 were expressed efficiently and at comparable levels (Figure 6A, B). Subsequently, we found that overexpressing PARP1-WT significantly reduced the migration and proliferation of A2780 cells, whereas overexpressing PARP1-K192A showed minimal impact (Figure 6C-F). In addition, overexpressing PARP1-WT significantly reduced the levels of Ki-67 (Figure 7A, B) and PCNA (Figure 7C, D), while PARP1-K192A overexpression had negligible effects. Finally, overexpressing of PARP1-WT significantly increased ROS levels (Figure 8A, B) and annexin V signals (Figure 8C, D), whereas PARP1-K192A overexpression had minimal influence.

2.4 PARP1 K192 lactylation downregulates ERK activity

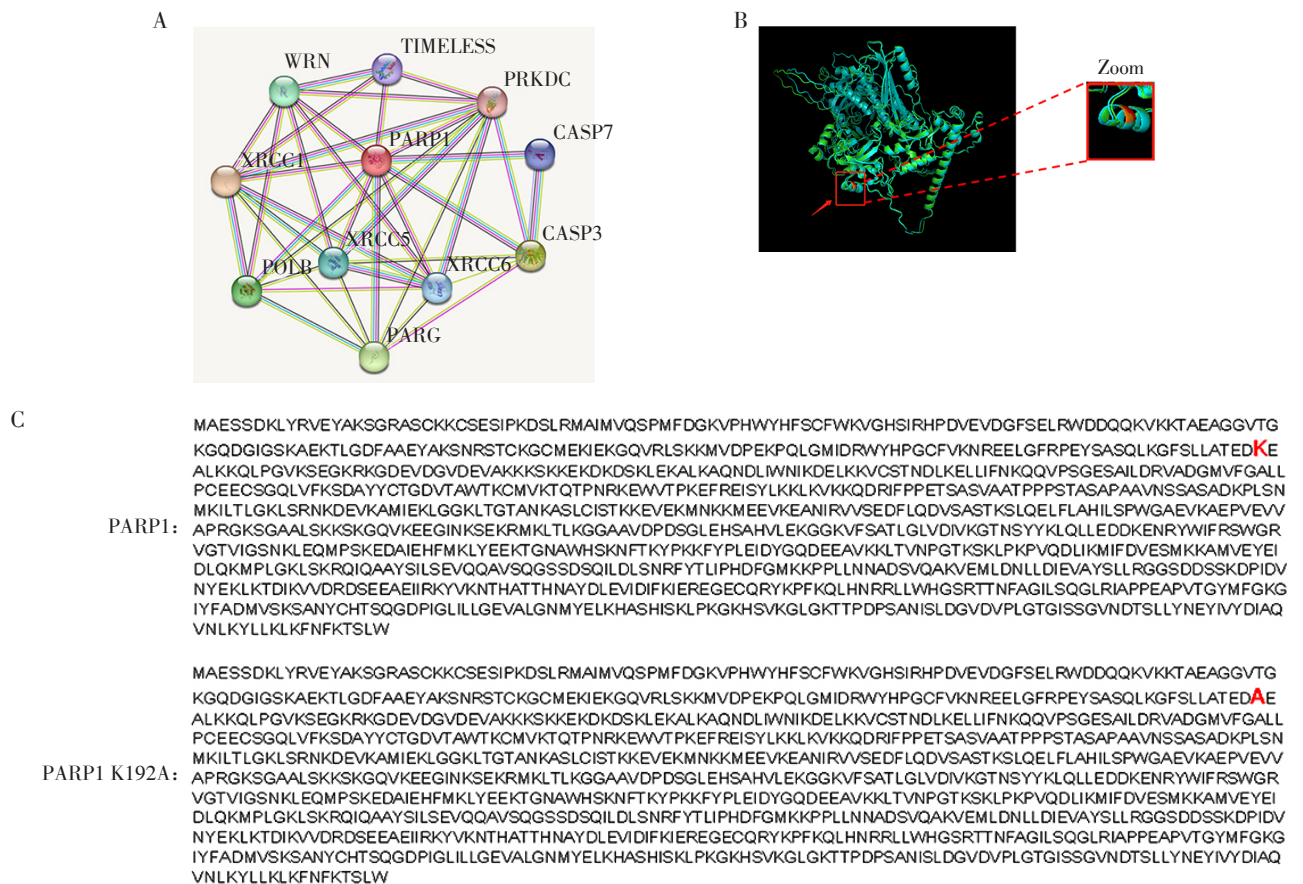
Next, we investigated whether PARP1 lactylation affected downstream oncogenic signals. We found that

overexpressing PARP1-WT significantly reduced p-ERK1/2 levels without altering gross ERK1/2 levels, while overexpressing PARP1-K192A had little effect (Figure 9A-D).

3 Discussion

This study is the first to comprehensively compare the levels of multiple pan-PTMs between female normal ovarian and OC samples. It revealed that pan-lactylation was the most upregulated PTMs and identified many DLP sites in OC samples. Moreover, it showed that lactylation of PARP1 at K192 might regulate OC progression and proliferation through the ERK1/2 pathway.

PARP1 is upregulated at both the messenger RNA (mRNA) and protein levels, with a concomitant increase in its enzymatic activity, in some cancers, in-



A: Protein interaction network analysis by String showed that PARP1 is at the center and had connection with each important oncoproteins. B: Structural prediction by Alphafold showed that K192A caused only a small shift. C: K192 sites and adjacent sequences in PARP1 is conserved between human and mouse.

图5 PARP1相互作用网络和结构预测

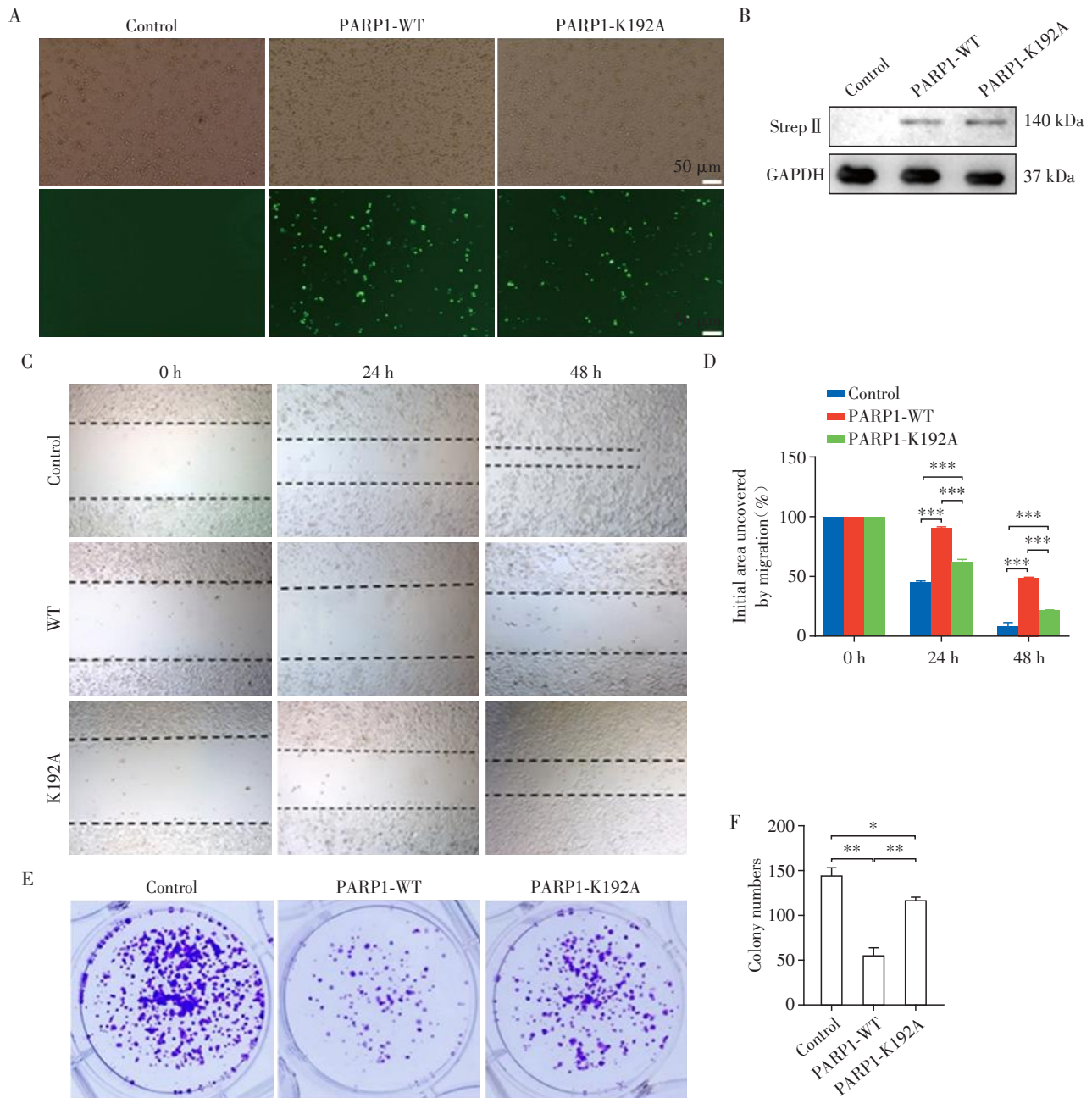
Figure 5 Interaction and structure prediction of PARP1

cluding primary prostate, and colorectal cancer^[19-21]. It is also overexpressed in other malignancies, such as endometrial adenocarcinoma, small - cell lung cancer, skin cancer, non-Hodgkin lymphoma, and triple-negative breast cancer^[22-24]. Moreover, various studies have shown that increased PARP1 levels correlate positively with tumor progression^[25-26]. However, unlike these studies, ours found that overexpressing PARP1 - WT suppressed the proliferation of OC cells. This difference might be because PARP1 is already expressed at a high level in A2780 cells, and its further overexpression places it in a hyper-activated state. PARP1 has been reported to caused intracellular exhaustion of NAD⁺ and ATP, which in turn induces cell necrosis and death. In addition, other reports have shown that PARP1 overactivation induces excessive PAR synthesis and induced apoptosis^[27-28]. Moreover, excessive

PARP1 induced PAR was shown to be directly toxic to neurons and trigger signals to induce neuron death^[14-29]. Our recent study also found that PARP1 overactivation suppressed the proliferation of cervical cancer cells^[14].

Our study examined multiple essential kinases regulating cancer cell progression A2780 cells overexpressing PARP1-WT or PARP1-K192A. Overexpressing PARP1-WT significantly reduced p-ERK1/2 levels, a well-known critical oncoprotein, which may be one mechanism by which overexpressing PARP1-WT reduced the proliferation of A2780 cells. Interestingly, PARP1 overactivation was found to promoted cell death by downregulating p-ERK1/2^[30].

Collectively, our study uncovered a new lactylation site on PARP1 in OC, which functions in OC progression. Further investigations are required to understand how lactylation regulates PARP1 function.



A, B: Fluorescence imaging(A) and Western blot(B) showed that either PARP1-WT-EGFP-strep II and PARP1-K192A-EGFP-strep II could be efficiently transfected into A2780 cells and expressed at a similar level (scale bar=50 μm.). C, D: Scratch assay on A2780 cell monolayers showed that PARP1-WT OE significantly decreased the closure rate of the scratched area, while PARP1- K192A/Q had much less impact. E, F. Colony formation assay showed that PARP1-WT OE significantly decreased the number of cell colonies formed by A2780 cells, while PARP1- K192A/Q had much less impact. * $P < 0.05$, ** $P < 0.01$ and *** $P < 0.001$ ($n=3$).

图6 PARP1 过表达降低了 A2780 细胞的迁移和克隆形成

Figure 6 PARP1 overexpression decreased migration and colony formation in A2780 cells

Data availability statement:

The data that support the findings of this study are available from the corresponding author upon reasonable request. Supplementary dataset 1 has been deposited into Zenodo (DOI: 10.5281/zenodo.8164720).

利益冲突声明:

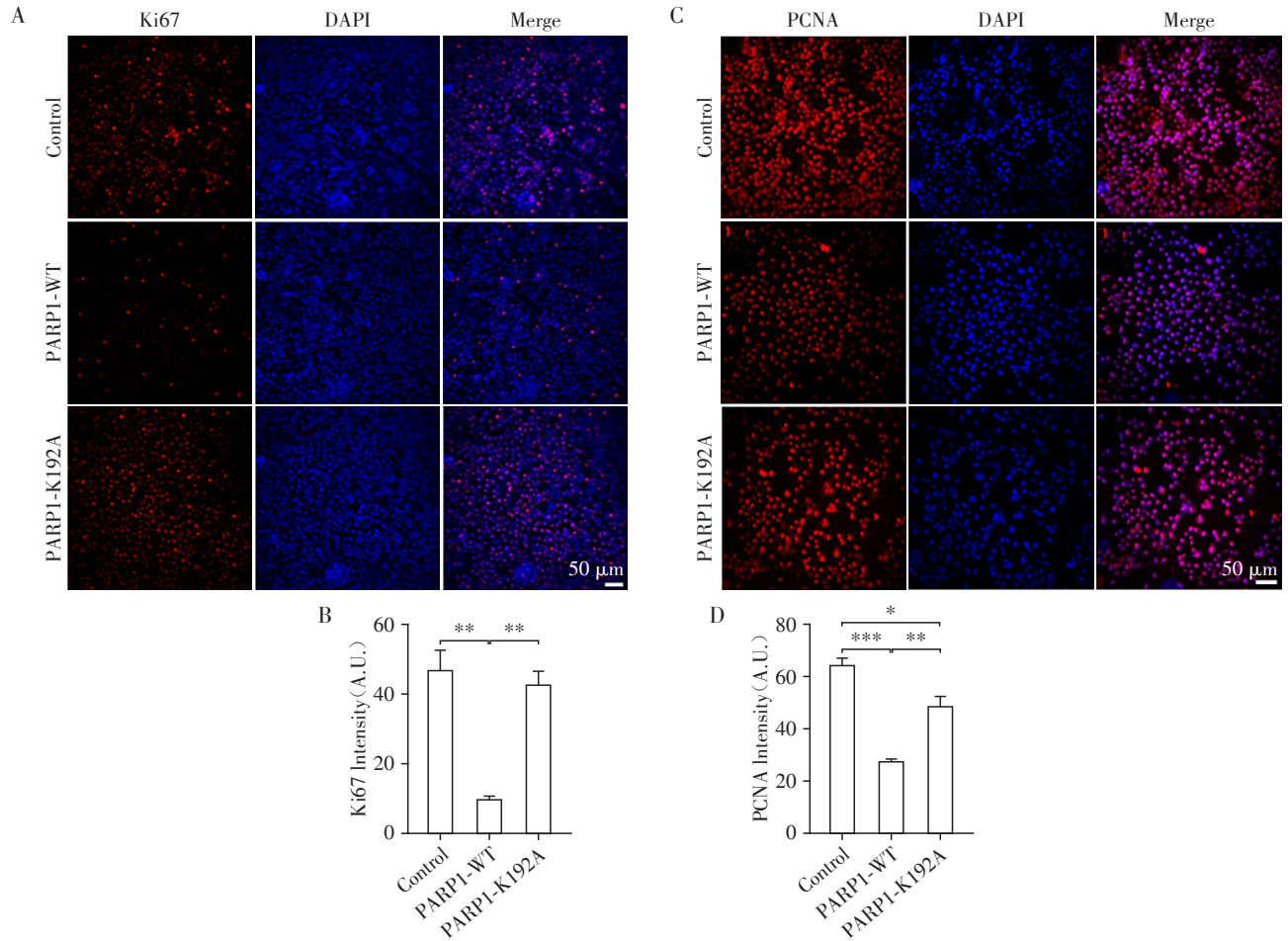
所有作者声明无利益冲突。

Conflict of Interests:

The authors declared that they have no conflicts of interest to this work.

作者贡献声明:

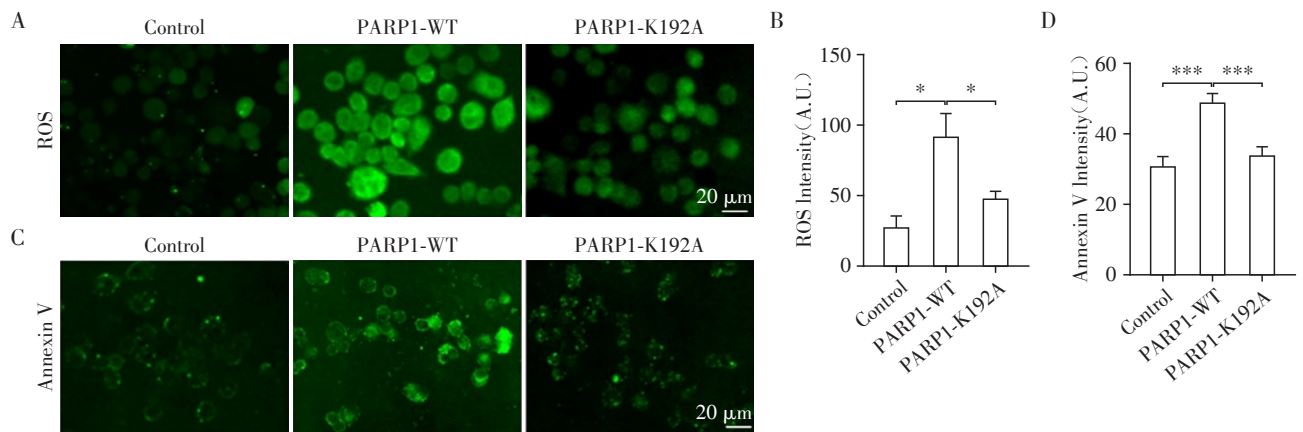
苏宁负责大部分实验操作、数据收集与分析工作;曹颖完成了诸多基础性工作(如临床样本采集、全蛋白翻译后修饰筛选等);张淑平参与实验操作、数据收集与分析工作;应



A-D: Immunofluorescence and quantification of Ki67(A and B), and PCNA(C and D) showed that PARP1-WT OE significantly decreased the proliferation of A2780 cells, while PARP1-K192A had much less impact. * $P < 0.05$, ** $P < 0.01$, and *** $P < 0.001$ (scale bar=50 μm , $n=3$).

图7 PARP1过表达降低了A2780细胞的增殖

Figure 7 PARP1 overexpression decreased proliferation of A2780 cells



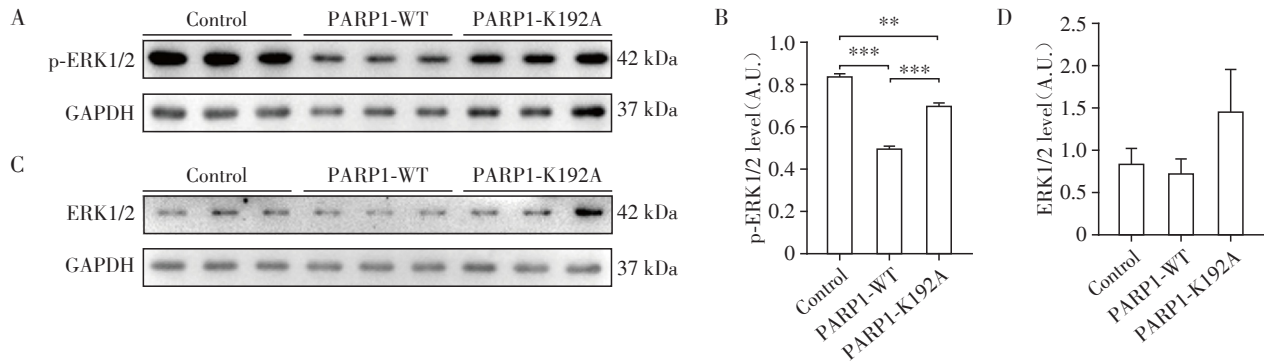
A, B: ROS staining and quantification showed that PARP1-WT OE significantly increased ROS level of A2780 cells, while PARP1-K192A had much less impact. C, D: Annexin V staining and quantification showed that PARP1-WT OE significantly increased the apoptosis level of A2780 cells, while PARP1-K192A had much less impact. * $P < 0.05$, *** $P < 0.001$ (scale bar=20 μm , $n=3$).

图8 PARP1过表达降低了A2780细胞的健康状况

Figure 8 PARP1 overexpression decreased health status of A2780 cells

小燕、杨莉莉和张东负责实验设计;其余作者均参与了部分实验协助工作。论文稿件由张东在苏宁协助下撰写,应小燕

和杨莉莉负责审核并提出修改建议。所有作者均阅读了论文终稿并同意发表。



A, B: Western blotting and quantification showed that PARP1 over expression significantly decreased p-ERK1/2. C, D: Western blotting showed the protein levels of ERK1/2 in Control, PARP1-WT, and PARP1-K192A were identical, with GAPDH as an internal control. ** $P < 0.01$ and *** $P < 0.001$ ($n=3$).

图9 PARP1过表达降低p-ERK1/2水平

Figure 9 PARP1 overexpression decreased p-ERK1/2

Author's Contributions:

SU Ning was the primary charger in most of the experiments, data collection and analysis, CAO Ying did many fundamental jobs (clinical sample collection, pan-PTM screen, etc); ZHANG Shuping made substantial contribution; YING Xiaoyan, YANG Lili, and ZHANG Dong designed the research; All others assisted in some of the experiments. ZHANG Dong wrote the manuscript with the assistance of SU Ning. YING Xiaoyan and YANG Lili proofread and gave advice. All authors read and approved the final manuscript.

[References]

- [1] SIEGEL R L, MILLER K D, WAGLE N S, et al. Cancer statistics, 2023 [J]. *CA A Cancer J Clin*, 2023, 73(1): 17-48
- [2] ZHANG R Q, SIU M K Y, NGAN H Y S, et al. Molecular biomarkers for the early detection of ovarian cancer [J]. *Int J Mol Sci*, 2022, 23(19): 12041
- [3] DENG H, ZHU H L, LI Y, et al. Treatment of liver metastases in patients with epithelial ovarian cancer [J]. *Chin Med J(Engl)*, 2021, 134(10): 1236-1238
- [4] WANG J Y, GROSS M, URBAN R R, et al. Intraperitoneal and hyperthermic intraperitoneal chemotherapy for the treatment of ovarian cancer [J]. *Curr Treat Options Oncol*, 2024, 25(3): 313-329
- [5] HE X F, HU X L, WEN G J, et al. O-GlcNAcylation in cancer development and immunotherapy [J]. *Cancer Lett*, 2023, 566: 216258
- [6] GEFFEN Y, ANAND S, AKIYAMA Y, et al. Pan-cancer analysis of post-translational modifications reveals shared patterns of protein regulation [J]. *Cell*, 2023, 186(18): 3945-3967
- [7] HE Y P, SONG T B, NING J Z, et al. Lactylation in cancer: Mechanisms in tumour biology and therapeutic potentials [J]. *Clin Transl Med*, 2024, 14(11): e70070
- [8] ZHANG D, TANG Z Y, HUANG H, et al. Metabolic regulation of gene expression by histone lactylation [J]. *Nature*, 2019, 574(7779): 575-580
- [9] JIANG J, HUANG D L, JIANG Y, et al. Lactate modulates cellular metabolism through histone lactylation-mediated gene expression in non-small cell lung cancer [J]. *Front Oncol*, 2021, 11: 647559
- [10] LI F, ZHANG H H, HUANG Y, et al. Single-cell transcriptome analysis reveals the association between histone lactylation and cisplatin resistance in bladder cancer [J]. *Drug Resist Updat*, 2024, 73: 101059
- [11] CUI H C, XIE N, BANERJEE S, et al. Lung myofibroblasts promote macrophage profibrotic activity through lactate-induced histone lactylation [J]. *Am J Respir Cell Mol Biol*, 2021, 64(1): 115-125
- [12] MENG X X, BAINE J M, YAN T C, et al. Comprehensive analysis of lysine lactylation in rice (*Oryza sativa*) grains [J]. *J Agric Food Chem*, 2021, 69(29): 8287-8297
- [13] JEONG K Y, LEE H. Inhibition of poly(ADP-ribose) polymerase: a promising strategy targeting pancreatic cancer with BRCAness phenotype [J]. *World J Gastrointest Oncol*, 2021, 13(11): 1544-1550
- [14] YANG L L, ZHANG X K, CAO Y, et al. PARP1 acetylation at K119 is essential in regulating the progression and proliferation of cervical cancer cells [J]. *Med Oncol*, 2024, 41(11): 273
- [15] WU Y S, XU S L, CHENG S S, et al. Clinical application of PARP inhibitors in ovarian cancer: from molecular mechanisms to the current status [J]. *J Ovarian Res*, 2023, 16(1): 6

(下转第1241页)

- tential[J]. *Mol Cancer*, 2020, 19(1): 127
- [20] WANG H, LIANG Y K, ZHANG T, et al. C-IGF1R encoded by cIGF1R acts as a molecular switch to restrict mitophagy of drug-tolerant persister tumour cells in non-small cell lung cancer [J]. *Cell Death Differ*, 2023, 30(11): 2365-2381
- [21] ROY R, HUANG Y Y, SECKL M J, et al. Emerging roles of hnRNPA1 in modulating malignant transformation [J]. *Wiley Interdiscip Rev RNA*, 2017, 8(6). DOI: 10.1002/wma.1431
- [22] ZHU W Z, TAN L L, MA T T, et al. Long noncoding RNA SNHG8 promotes chemoresistance in gastric cancer *via* binding with hnRNPA1 and stabilizing TROY expression [J]. *Dig Liver Dis*, 2022, 54(11): 1573-1582
- [23] CHEN L Q, ZENG Y, REN B Q, et al. ALDOC regulated the biological function and immune infiltration of gastric cancer cells [J]. *Int J Biochem Cell Biol*, 2023, 158: 106407
- [收稿日期] 2025-04-29
(本文编辑: 唐 震)

(上接第 1228 页)

- [16] ZHAO Y, ZHANG L X, JIANG T, et al. The ups and downs of poly (ADP-ribose) polymerase-1 inhibitors in cancer therapy-Current progress and future direction [J]. *Eur J Med Chem*, 2020, 203: 112570
- [17] GUPTA R, KUMAR P. Computational analysis indicates that PARP1 acts as a histone deacetylases interactor sharing common lysine residues for acetylation, ubiquitination, and SUMOylation in Alzheimer's and Parkinson's disease [J]. *ACS Omega*, 2021, 6(8): 5739-5753
- [18] LAGUNAS V M, MELÉNDEZ-ZAJGLA J. Nuclear factor-kappa B as a resistance factor to platinum-based antineoplastic drugs [J]. *Met Based Drugs*, 2008, 2008: 576104
- [19] HUANG M Q, CHEN L, GUO Y C, et al. PARP1 negatively regulates transcription of BLM through its interaction with HSP90AB1 in prostate cancer [J]. *J Transl Med*, 2023, 21(1): 445
- [20] ZHANG G Y, WANG Z M, BAVARVA J, et al. A recurrent ADPRHL1 germline mutation activates PARP1 and confers prostate cancer risk in African American families [J]. *Mol Cancer Res*, 2022, 20(12): 1776-1784
- [21] XU K W, YU Z G, LU T L, et al. PARP1 bound to XRCC2 promotes tumor progression in colorectal cancer [J]. *Discov Oncol*, 2024, 15(1): 238
- [22] BYERS L A, WANG J, NILSSON M B, et al. Proteomic profiling identifies dysregulated pathways in small cell lung cancer and novel therapeutic targets including PARP1 [J]. *Cancer Discov*, 2012, 2(9): 798-811
- [23] BI F F, LI D, YANG Q. Hypomethylation of ETS transcription factor binding sites and upregulation of PARP1 expression in endometrial cancer [J]. *Biomed Res Int*, 2013, 2013: 946268
- [24] ROJO F, GARCÍA-PARRA J, ZAZO S, et al. Nuclear PARP-1 protein overexpression is associated with poor overall survival in early breast cancer [J]. *Ann Oncol*, 2012, 23(5): 1156-1164
- [25] YANG X D, KONG F N, QI L, et al. PARP inhibitor olaparib overcomes sorafenib resistance through reshaping the pluripotent transcriptome in hepatocellular carcinoma [J]. *Mol Cancer*, 2021, 20(1): 20
- [26] WANG F F, GOUITIA O G, WANG L, et al. PARP1 upregulation in recurrent oral cancer and treatment resistance [J]. *Front Cell Dev Biol*, 2022, 9: 804962
- [27] CHEN L, ZOU Y H, SUN R H, et al. Minimizing DNA trapping while maintaining activity inhibition *via* selective PARP1 degrader [J]. *Cell Death Dis*, 2024, 15(12): 898
- [28] RAMESH S, ALMEIDA S D, HAMMIGI S, et al. A review of PARP-1 inhibitors: assessing emerging prospects and tailoring therapeutic strategies [J]. *Drug Res (Stuttg)*, 2023, 73(9): 491-505
- [29] FOSSATI S, CIPRIANI G, MORONI F, et al. Neither energy collapse nor transcription underlie *in vitro* neurotoxicity of poly (ADP-ribose) polymerase hyper-activation [J]. *Neurochem Int*, 2007, 50(1): 203-210
- [30] ETHIER C, LABELLE Y, POIRIER G G. PARP-1-induced cell death through inhibition of the MEK/ERK pathway in MNNG-treated HeLa cells [J]. *Apoptosis*, 2007, 12(11): 2037-2049
- [收稿日期] 2024-11-19
(本文编辑: 戴王娟)